Current Topics in Electrochemistry
Vol. 17, 2012

Original Communication

# Determination of cobalt-pilocarpine complex with mercury modified gold quartz crystal microbalance electrode

**Lai-Hao Wang* and Yi-Chieh Li**

Department of Medical Chemistry, Chia Nan University of Pharmacy and Science, 60 Erh-Jen Road, Section 1, Jen Te, Tainan 71743, Taiwan

## ABSTRACT

Mercury films on gold/quartz electrodes were prepared using a potentiostatic method and a potentiodynamic method: the repeated cyclic voltammetry technique. The film formation was confirmed using the electrochemical quartz crystal microbalance method; 17 μg of mercury film was deposited per cycle. The electrochemical deposition of mercury film on the gold/quartz substrate was evaluated with respect to a quartz crystal microbalance cell, deposition time, and the concentration of mercury. Electrochemical studies have shown that cobalt (II), pilocarpine, and a cobalt-pilocarpine complex are catalytically reduced more efficiently on a mercury-modified gold/quartz electrode than on a bare gold/quartz electrode. In addition, atomic force microscopy images clearly showed the structure of the adsorbed cobalt-pilocarpine complex molecule layers on mercury-modified gold/quartz electrode.

**KEYWORDS:** QCM cell, modified gold/quartz electrode, cobalt-pilocarpine

## 1. INTRODUCTION

Pilocarpine {2(3H)-Furanone, 3-ethyldihydro-4-[(1-methyl-1H-imidazol-5-yl) methyl]-} is widely used to treat glaucoma, especially the acute form of angle-closure glaucoma. Pilocarpine forms complexes with metals such as $Ca^{2+}$, $Mg^{2+}$, $Cu^{2+}$, and $Co^{2+}$. The formation of pilocarpine-metal complexes is probably involved in the pharmacologic mechanisms of the drug [1-9].

Electrodes using mercury coated substrates (glassy carbon, gold, and platinum) have been used for analysis [10-14]. A significant attribute of the electrochemical quartz crystal microbalance (also called "electrochemical quartz crystal microgravimetry"; EQCM) method is that it provides correlations between electrochemically induced mass changes on the electrode surface and the charge consumed in the process. Such measurements aid in determining the composition of the deposit, its stoichiometry, and the efficiency of the usage of charge in its deposition [15]. EQCM is ideally suited for the study of metal deposition reactions. However, very few reports [16, 17] focus on the influence of mercury films on substrates for EQCM. Voltammetric and EQCM techniques have been used to examine the complexation ligand with metal [18-23]. There are no published reports on depositing mercury onto a gold-coated quartz electrode to study the Co (II) - pilocarpine complex. The aim of the present study was to design a horizontally or vertically joined quartz crystal microbalance (QCM) cell holder for the deposition of mercury onto a gold/quartz electrode, and describe how a mercury layer is electrodeposited on the electrode surface of the crystal. Mercury film-based gold/quartz electrode was used as a working electrode to catalyze the electroreduction of the Co (II) - pilocarpine complex.

*Corresponding author: e201466wang@msa.hinet.net

## 2. EXPERIMENTAL

### 2.1. Materials and apparatus

A Co (II)-pilocarpine complex was prepared using a previously reported method [1]. Other chemical reagents used were of analytical grade. The EQCM system used for experiments consisted of a potentiostat/galvanostat (263A; EG&G Princeton Applied Research, Princeton, NJ, USA) coupled to a quartz crystal analyzer (QCA 922; Seiko EG&G Co., Ltd., Chiba, Japan). The QCM cell was homemade and connected to a well-type quartz crystal holder (QA-CL4; Seiko). The crystal was mounted in the holder and connected with an adapter cable (QCA 922-10; Seiko). A schematic of the experimental setup is shown in Scheme 1. When the quartz crystal was immersed in the solution, only one side of it was exposed to the electrolyte solution; that side was used as the sensing surface that enabled measurements of small changes in mass and viscosity of the liquid. A 9-MHz quartz crystal with a 300-nm layer of gold sputtered onto a 100-nm layer of titanium used for the working electrode substrate (geometric area: 0.196 $cm^2$) was also purchased from Seiko. A platinum wire counter and an Ag/AgCl reference electrode (RE-1; Bioanalytical Systems, Inc. (BAS), West Lafayette, IN, USA) completed the electrochemical set-up (Scheme 1). The gray and flat part beneath the balls also deposited Hg particles on gold/quartz electrode.

### 2.2. Preparing thin-film mercury on a gold/quartz surface for EQCM

Mercury was deposited potentiostatically onto the gold electrode of the quartz using the following three methods: (1) the gold/quartz electrode was placed in the solution (Scheme 2A); (2) the QCM cell (special vessel device) was attached horizontally to the flanges of the holder and a vessel with a clip (Scheme 2B); (3) the QCM cell was attached vertically to the front of the holder and a vessel with a clip (Scheme 2C). The gold/quartz electrode was exposed to 0.1 M

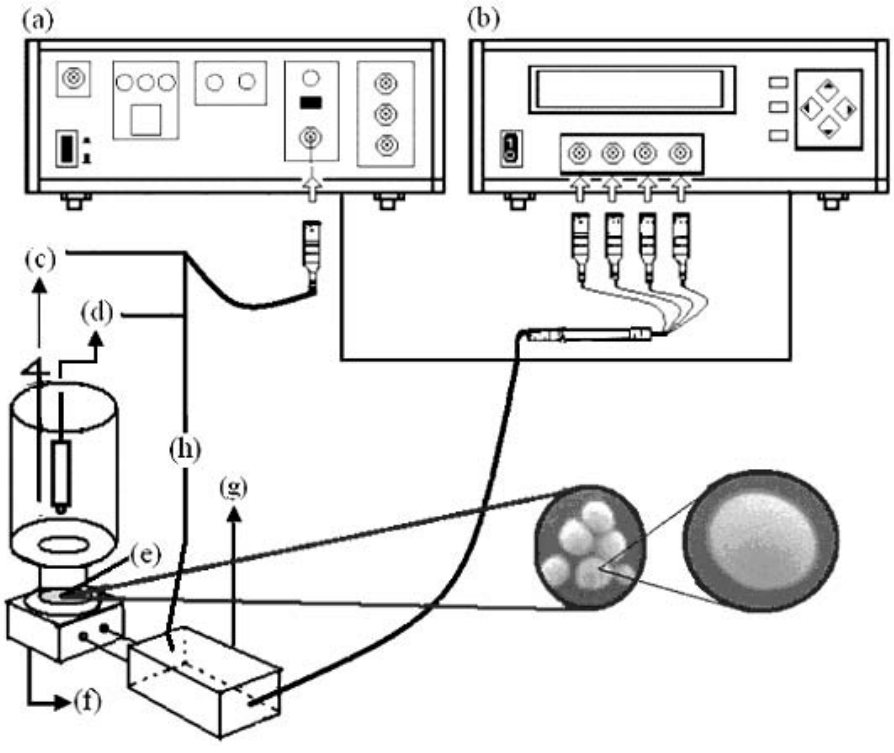


**Scheme 1.** Schematic representation of the experimental set up (QCM cell was home-made). (a) potentiostat/galvanostat; (b) quartz crystal analyzer; (c) platinum counter electrode; (d) Ag/AgCl reference electrode; (e) Hg modified Au/quartz working electrode; (f) quartz crystal holder; (g) adapter cable; (h) terminal for connecting working electrode.

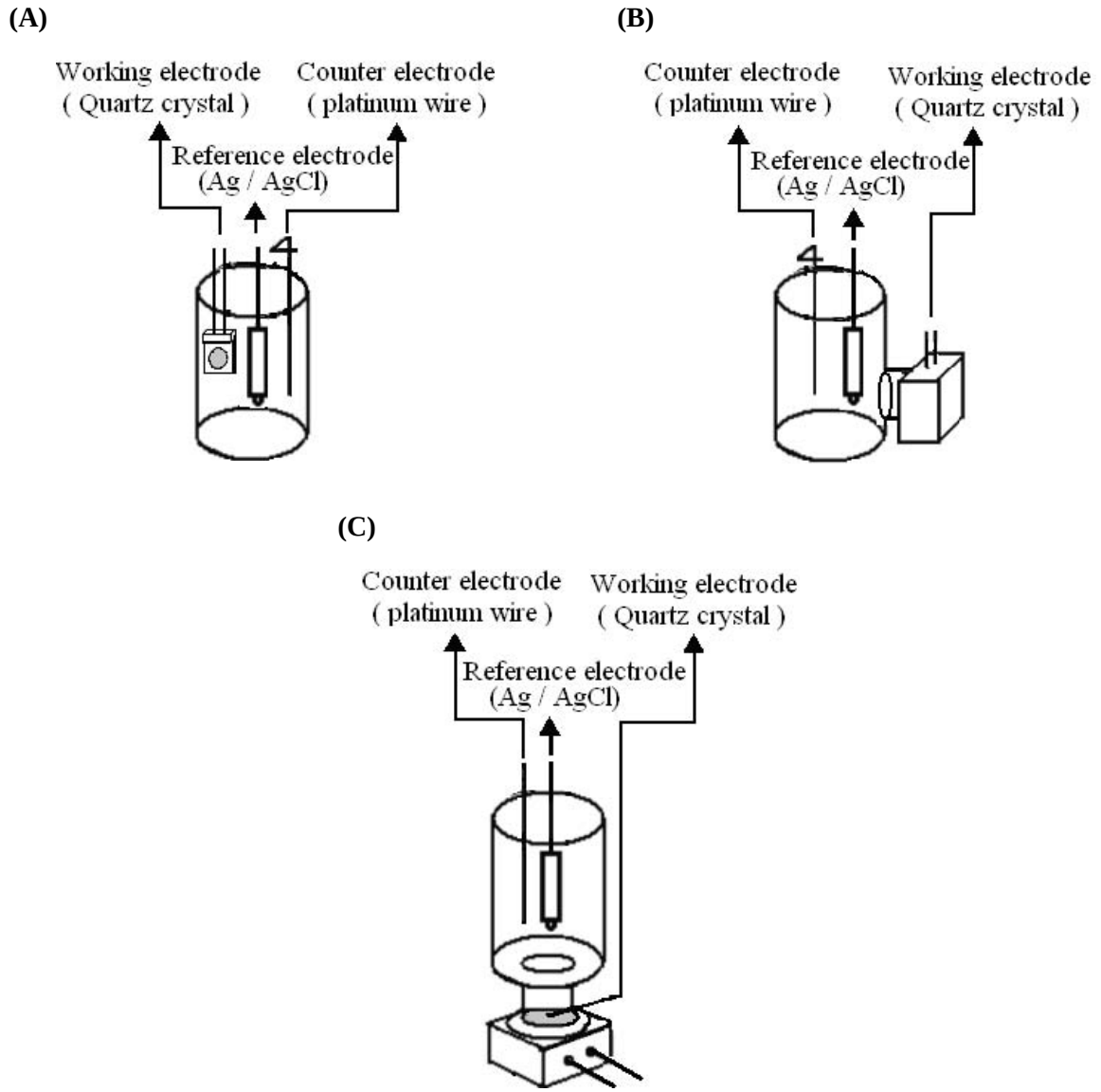


**Scheme 2.** QCM cell devices for deposition mercury films on Au/quartz.

acetate buffer that contained Hg $(NO_3)_2$, and the resonance frequency of the quartz was monitored. The electrodeposition of mercury was under potentiostatic conditions at –1.0 V and 2, 4, and 8 min, respectively, and the deposition behavior of the mercury was checked using differential pulse voltammetry at 10 mV/s. The QCM crystal was covered with a thin layer of mercury and was subjected to subsequent voltammetric studies. Cyclic voltammograms were taken of Co (II), pilocarpine, and the Co (II)-pilocarpine complex accumulated on the mercury- and gold-coated quartz crystal between 0.0 V and –1.8 V in lithium perchlorate (pH 6.01). Cyclic voltammetry was done on a gold-coated QCM in order to monitor the mass change of the electrode concurrently with the electrochemical measurements.

## 3. RESULTS AND DISCUSSION

### 3.1. Choice of electrodeposition conditions

#### 3.1.1. Effect of QCM device methods

For comparison, thin films of mercury were deposited on the gold/quartz electrode. From

Table 1 and 2, it can be seen that, the QCM cell contained the acetate solution and a 2.0-mM concentration of Hg $(NO_3)_2$, and was connected either vertically or horizontally to the gold/quartz crystal at a scan rate of 10 mV/s and a deposition time of 240 s (Scheme 2). We compared EQCM and voltammetric data using the equation:

$$i(t) = -\frac{knF}{AM} \bullet \frac{d\Delta f}{dt} ,$$

where $M$ is the molar mass of deposited metal, $n$ is the number of electrons transferred to the metal ion, $F$ is Faraday's constant, $A$ is the electrochemically active area, $f$ is the frequency, and $t$ is the time. The sense of $k$ is evident from the equation: $\Delta m = -k\,\Delta f$.

Table 1 compares the mass changes during mercury deposition on the gold/quartz electrode. The change in weight, $\Delta m$, was calculated from the change in frequency, $\Delta f$, using the Sauerbrey equation [24]. We found that the mass change caused by method (3) was higher than that of the other methods tested because the cell system (C) provided for a uniform current density distribution over the surface of the working electrode.

**Table 1.** Effect of QCM cell design methods of deposition mercury on Au/quartz electrode.

| Methods | Mass changes (μg) |
|---|---|
| 1 | - [a] |
| 2 | 4.640 ± 0.372 |
| 3 | 16.945 ± 2.997 |

Mercury concentration: 2.0 mM; scan rate: 10 mV/s; deposition time: 240 s
- [a]: Not mass change

**Table 2.** Effect of mercury concentration of mercury deposition on Au/quartz electrode.

| Mercury concentration | Mass changes (μg) |
|---|---|
| 0.5 mM | 9.02 |
| 1.0 mM | 24.4 |
| 2.0 mM | 42.0 |
| 4.0 mM | 42.5 |

Scan rate: 10 mV/s; deposition time: 480 s; Method: (3)

Therefore, we did electrochemical deposition experiments in which we vertically connected the QCM cell with the gold/quartz electrode in a vertical direction.

### 3.1.2. Effect of deposition time

For comparison, we determined the frequency change (Δf) of scan rate (10 mV, 25 mV and 50 mV), rotation rate, and scan order (from the first to the fifth scan) of the Hg deposited on the gold/quartz electrode. The decreased amount of mass changes of deposited Hg (II) were calculated to be 5890-2210 ng with scan rate, and 17960-13200 ng with scan order, respectively. Therefore, the first scan at rate 10 mV/s was chosen for use in the deposition of 2.0 mM Hg (II). The linear response of frequency change against the electrode potential occurred because the Hg deposition had finished; and frequency changes were found to be 21410 Hz for 240 s and 39800 Hz for 480 s, respectively, between 0.0 V and -1.0 V *vs* Ag/AgCl, which indicate a decrease of Hg (II) species. The mercury film was electrochemically deposited for 240 s and 480 s, which yielded mass changes of about 16.9 μg and 29.3 μg, respectively. For comparison, we determined frequency change ($\Delta f$) with scan number and scan method (from first to third scan) of the Hg deposited on the Au/quartz electrode. Using a cyclic voltammetry scan between −1.0 V and 0.0 V at 10 mV/s, we calculated the amount of deposited mercury to be 16.7 μg from the frequency change on the gold/quartz crystal electrode per cycle; this mass change was close to the amount of mercury deposited in 240 s. The mass change of 16.7 μg corresponds to the deposition of a 62-nm-thick mercury film.

### 3.1.3. The effect of various Hg (II) concentrations

A thin mercury film was electrodeposited onto the gold/quartz crystal using an acetate solution that contained varying concentrations of Hg $(NO_3)_2$ at a scan rate 10 mV/s for deposition time 480 s. We found that Hg (II) concentrations of 0.5 mM, 1 mM, 2.0 mM, and 4.0 mM resulted in mass changes of approximately 9.02 μg, 24.4 μg, 42.0 μg, and 42.5 μg, respectively, and that concentration of 2.0 mM and 4.0 mM resulted in the same mass change of approximately 42.0 μg. We therefore conclude that it is suitable for use of an Hg (II)

concentration of 2.0 mM. Energy dispersion spectroscopy (EDS) was used to study the elemental composition of material surfaces, and it showed a peak for Au (48 At %) and Hg (51 At %) as in Fig. 1. Field emission scanning electron microscope (FE-SEM) (JSM-7000; JEOL, Akishima City, Tokyo, Japan) photos of mercury deposited on the gold/quartz crystal electrode are shown in Fig. 1; the mercury diameter is between 300 nm and 500 nm.

### 3.2. The behavior of Co (II), pilocarpine, and Co (II)-pilocarpine on a Hg/Au/quartz electrode

To compare the electroanalytical utility of Au/quartz and modified Hg/Au/quartz electrodes, we measured the cyclic voltammograms (CV) of the Co (II)-pilocarpine on different electrodes in 0.1 M of $LiClO_4$. The Hg/Au-coated electrode performed better than the Au/quartz electrode (Fig. 2), and was used to evaluate Co (II), pilocarpine, and the Co (II)-pilocarpine complex. The Co (II) at mercury electrode was catalyzed by imidazole compounds; a mechanism for the electrocatalytical reaction had been proposed [25]. The Co (II) complex background potential of almost -0.2 V is closely related to the redox potential of the Co (III)/Co (II) couple is 0.2 V *vs* Ag/AgCl and the ligand reduction is mainly azo centred [26].

Fig. 3 shows a typical cyclic voltammogram and a frequency change-potential response ($\Delta f$-$E$ plot) on an Hg/Au/quartz electrode in the potential region between 0.0 and –1.8 V in $LiClO_4$ solution with 4.8 mM of the Co (II)-pilocarpine. We assumed that no adsorbed species existed on the surface at –1.0 V in solution, because the frequency reached a constant maximum value at that potential. A cathodic current for the Co (II)-pilocarpine was observed when the electrode potential exceeded –0.9 V. The potential was swept to more negative values, the current increased to a maximum of about –1.33 V, and the resonance frequency of the QCM decreased, which showed an increase in the surface mass or adsorption of the adsorbed species. We also found a reduction peak and a corresponding frequency

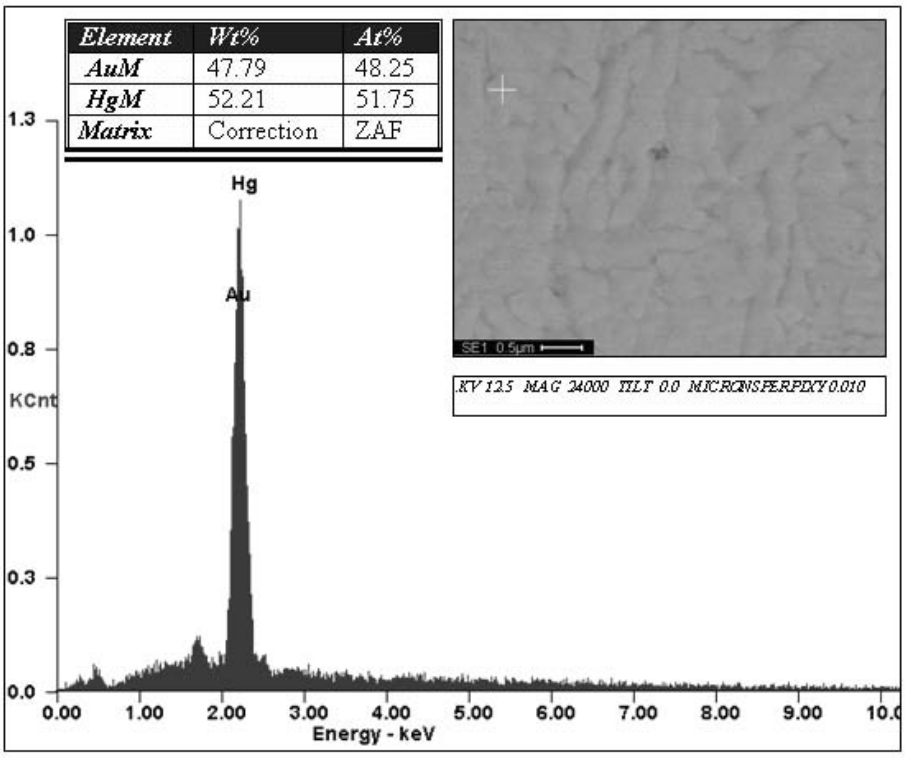


**Fig. 1.** Energy dispersion spectroscopy (EDS) and Scanning Electron Micrographs (SEM) of Hg/Au electrode.

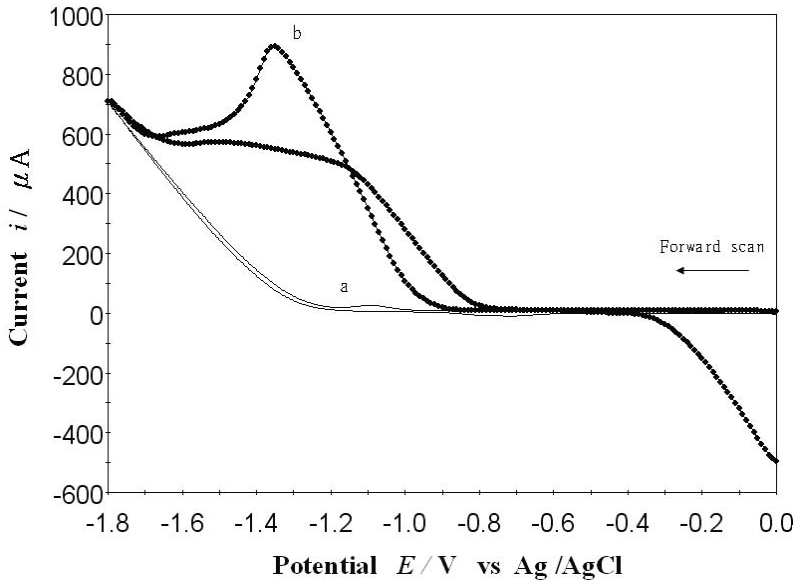


**Fig. 2.** Cyclic voltammograms of the Co(II)-pilocarpine complex (4.08 mM) on different electrodes in 0.1 M $LiClO_4$: (a) solid line, Au/quartz crystal electrode; (b) solid circle, modified Hg/Au/quartz crystal electrode. Scan rate: 25 mV/s.

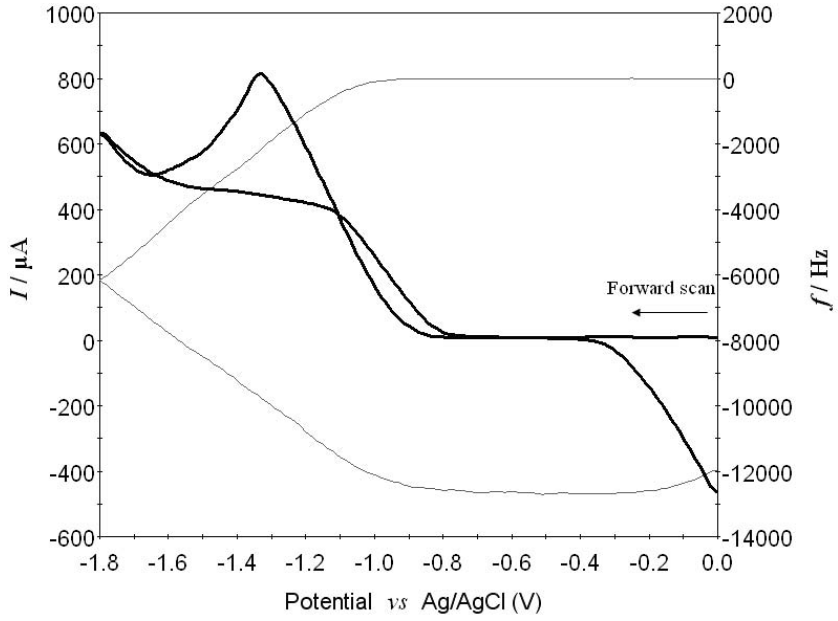


**Fig. 3.** Potentiodynamic simultaneous recording of current-potential and frequency of Co-pilocarpine (4.8 mM) in lithium perchlorate solution with scan rate at 25 mV/s on a modified Hg film/Au quartz crystal electrode.

decrease (Fig. 3). The mass continues to increase until the potential is reached and only at about -1.0 V does dissolution commence in accordance with the CV (Fig. 3).

In the parallel recorded frequency change response (Fig. 4), pronounced reversible frequency changes are found between the initial time (ca. 40 s) and the final time (110 s), but

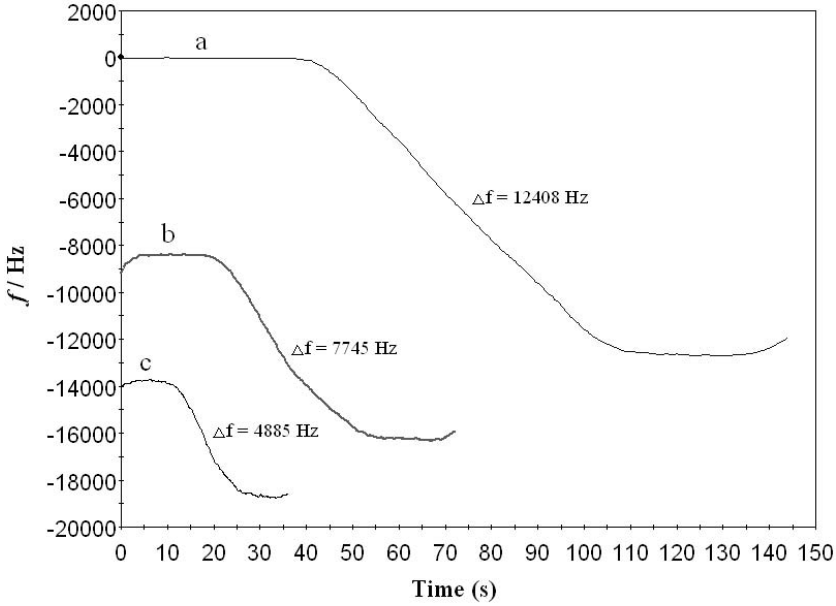


**Fig. 4.** Frequency shifts, $\Delta f$ ~$t$ (s) of Co-pilocarpine (4.8 mM) on the Au quartz crystal coated in lithium perchlorate solution with mercury at various scan rate (a) 25 mV/s; (b) 50 mV/s; (c)100 mV/s.

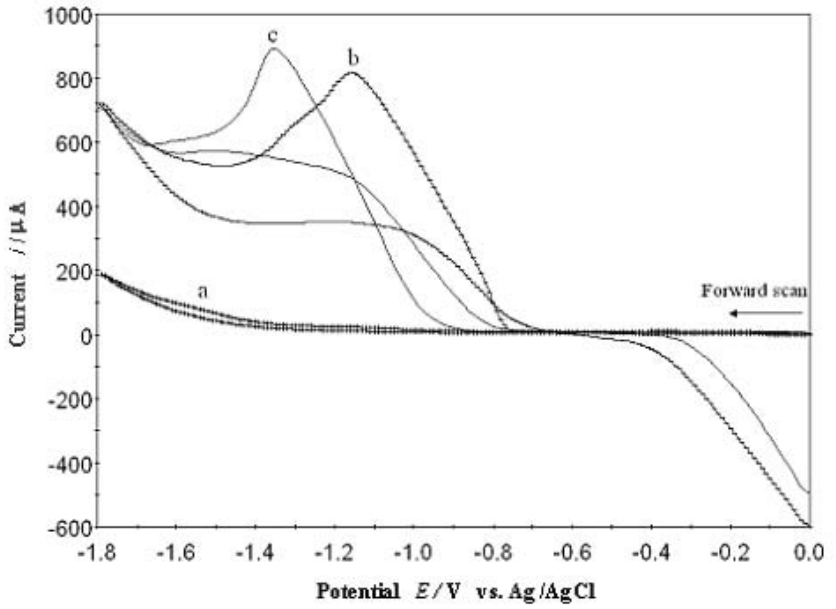


**Fig. 5.** Comparison of (a) pilocarpine; (b) Co(II); and (c) the Co(II)-pilocarpine complex. Scan rate: 25 mV/s on a modified Hg/Au/quartz crystal electrode.

between 45 and 105 s the change is very fast (negative frequency). The frequency decreased i.e., the mass on the electrode increased with time at a scan rate of 25 mV/s. The plot of $\Delta f$-$t$(s), $\Delta f_{110}$, is lower than that of $\Delta f_{0,}$ which is an indication that frequency decreased during the CV process, which means that the Co (II)-pilocarpine complex was adsorbed onto the electrode. The shapes of $\Delta f$ *versus* time curves can be interpreted using the adsorption-desorption mechanism of

the reduction process [13, 15]. The initial period corresponding to the potential plateau and increase on the electrode mass represent an adsorption period. The stage with decreasing potential and mass then corresponds to the adsorption.

The CV of pilocarpine in 0.1 M $LiClO_4$ shows no peak (Fig. 5, a) because it was not adsorbed by the mercury/gold/quartz electrode; however, Co (II) and the Co (II)-pilocarpine complex show reduction peaks at –1.16 V for Co (II) and –1.35 V for Co (II)-pilocarpine (Fig. 5, a and b), respectively. The formation of the Co (II)- pilocarpine complex is evident as the peak potential gets shifted to more negative side from -1.12 V to -1.35 V. Table 3 shows the mass changes of pilocarpine, Co (II), and the Co (II)-pilocarpine complex at various scan rates; the order of the mass changes is the Co (II)-pilocarpine complex > Co(II) > pilocarpine. That the reduction peak and mass change were much smaller for pilocarpine than for Co (II) and the Co (II)-pilocarpine complex means that pilocarpine was very weakly adsorbed on the mercury/gold/quartz electrode (Fig. 5 and Table 2). The Co (II)-pilocarpine complex was better adsorbed than were Co (II) and pilocarpine (Table 2); therefore, the mercury/gold/quartz electrode was used to detect the Co (II)-pilocarpine complex. The fact that in a solution with a small concentration of pilocarpine concentration the peak current of Co (II) is directly proportional to the concentration of pilocarpine was applied for analytical purposes. The polarographic wave of the Co (II)-pilocarpine complex has a diffuse character, which makes it ideal for measuring the levels of pilocarpine [7]. In the proposed conditions (Co (II) concentration = 4.08 mM, 0.1 M $LiClO_4$ solution, recoding of voltammograms from –1.12 V to –1.33 V), the concentrations of pilocarpine may range from 0.384 mM to 4.79 mM.

**Table 3.** Mass change of pilocarpine Co (II), and Co (II)- pilocarpine complex at various scan rate.

| Scan rate | Mass change (μg) | | |
|---|---|---|---|
| (mV/s) | Co(II) | Pilocarpine | Co-pilocarpine complex |
| 25 | 2.892 | 0.486 | 12.955 |
| 50 | 2.272 | 0.099 | 7.169 |
| 100 | 1.778 | 0.060 | 5.268 |

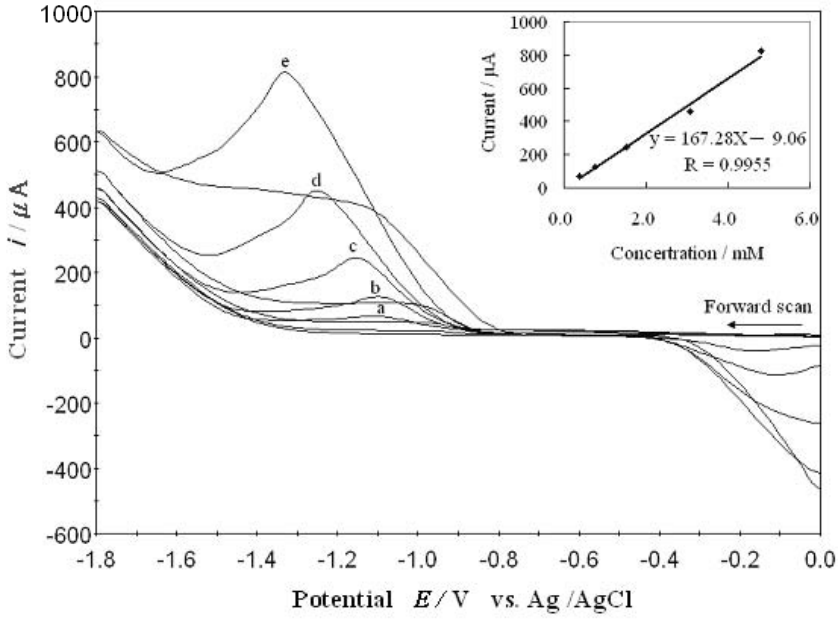


**Fig. 6.** Various concentrations of the Co(II)-pilocarpine complex: (a) 0.384 mM, (b) 0.767 mM, (c) 1.535 mM, (d) 3.07 mM, and (e) 4.79 mM, in 0.1 mole of $L^{-1}$ $LiClO_4$ solution. Scan rate: 25 mV/s on a modified Hg/Au/quartz crystal electrode.

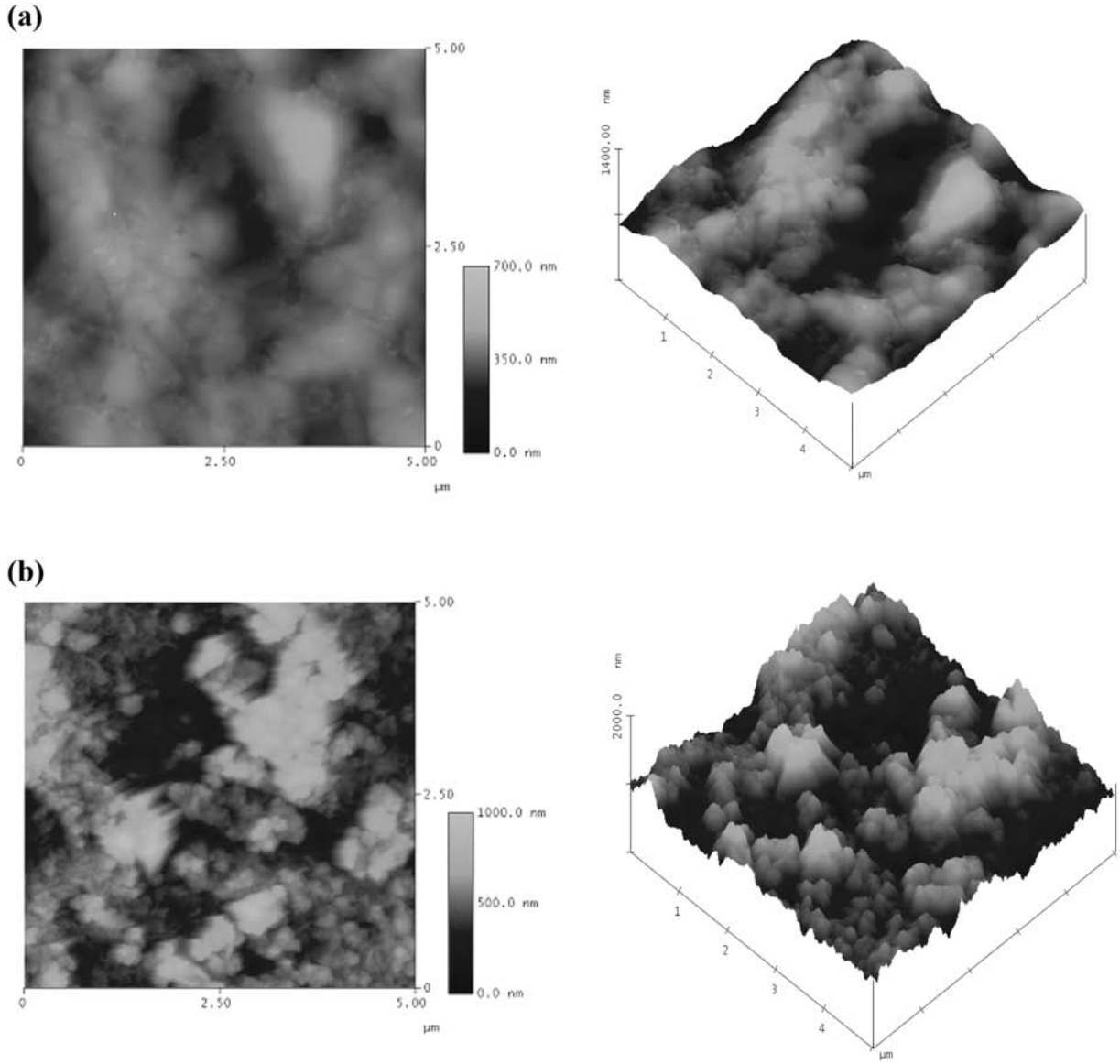


**Fig. 7.** Atomic force microscope (AFM) 2D and 3D images of (a) Hg (2 mM)/Au/quartz; (b) the Co(II)-pilocarpine complex Hg/Au/quartz.

Fig. 6 shows voltammograms for the reduction of different concentrations of the Co (II)-pilocarpine complex [0.384 mM-4.80 mM], which show increases in reduction peak current. In the inset, there is a linear plot of current against concentration [the regression equation used was ($y = 167x + 9.06$; correlation coefficient ($r$) = 0.9955)], which indicates that the peak current can be used to deduce concentration.

Fig. 7 shows representative atomic force micrographs comparing mercury/gold/quartz electrodes without (Fig. 7a) and with (Fig. 7b) the Co (II)-pilocarpine complex. The electro-adsorbed the Co (II)-pilocarpine complex formed an island on a mercury/gold/ quartz nano-composite electrode (Fig. 7b).

## CONCLUSIONS

We showed the EQCM responses from cyclic voltammograms for a mercury electrodeposition system on Au/quartz crystal electrodes. The Hg/Au/QCM electrode as well as sensitive and dynamic piezoelectric sensors were used to evaluate

the processing of Co (II), pilocarpine, and the Co (II)-pilocarpine complex, as well as sensitive and dynamic piezoelectric sensors.

## ACKNOWLEDGMENTS

This work was supported by grant NSC 94-2113-M-041-001 from the National Science Council, Taiwan.

## REFERENCES

1. Wang, L. H. and Li, Y. H. 2008, Curr. Pharmaceut. Anal., 4, 33.
2. Wisser, B. and Janiak, C. 2007, Z. Anorg. Allg. Chem., 633, 1796.
3. Guo, Y. and Jiang, L. 2006, Shiyong Erke Linchuang Zazhi (J. Appl. Clin. Pediatr.), 21, 490.
4. Gaggelli, E., Gaggelli, N. and Valensin, G. 1994, Met-Based Drugs, 1, 279.
5. Lenarcik, B. and Wisniewski, M. 1983, Pol. J. Chem., 57, 735.
6. Canti, G., Scozzafava, A., Ciciani, G. and Renzi, G. 1980, J. Pharm. Sci., 69, 1220.
7. Gromek, K. 1984, Chem. Anal., 29, 387.
8. Nasseh, I. E., Amado, D., Cavalheiro, E. A., Naffah-Mazzacoratti, M. G and Tengan, C. H. 2006, Epilepsy Res., 68, 229.
9. Bausch, S. B., Garland, J. P. and Yamada, J. 2005, Brain Res., 1045, 38.
10. Wang, L. H., Hsia, H. C. and Lan, Y. Z. 2006, Sensors, 6, 1555.
11. O'Shea T. J. and Lunte, S. M. 1993, Anal. Chem., 65, 247.
12. Allison,L. A. and Shoup, R. E. 1983, Anal. Chem., 55, 8.
13. Wang, Y., Zhu, G. and Wanf, E. 1997, Anal. Chim. Acta, 338, 97.
14. Andersen, N. P. R. 1998, Anal. Chim. Acta, 368, 191.
15. Ward, M. D. and Buttry, D. A. 1999, Science, 249, 1000.
16. Evans, C. D., Nicic, I. and Chambers, J. Q. 1995, Electrochim. Acta, 40, 2611.
17. Cho, K., Yoon, S., Jung, M. C. and Kim, H. 1998, Colloids Surf. A: Physicochem. Eng. Asp., 134, 59.
18. Nigam, P., Mohan, S., Kundu, S. and Prakash, R. 2009, Talanta, 77, 1426.
19. Vaskelis, A., Stankeviciene, I., Jagminiene, A., Tamasiunaite, L. T. and Norkus, E. 2008, J. Electroanal. Chem., 622, 136.
20. Viel, P., Dubois, L., Lyskawa, J., Sallé, M. and Palacin, S. 2007, Appl. Surf. Sci., 253, 3263.
21. Sezer, E., Esma, H. and Heinze, J. 2006, Electrochim. Acta, 51, 3668.
22. Inzelt, G., Puskas, Z., Nemeth, K. and Varga, I. 2005, J. Solid State Electrochem., 9, 823.
23. Sun, L. and Villemure, G. 2004, Clays Clay Miner., 52, 31.
24. Sauerbrey, G. 1959, Z. Phys., 155, 206.
25. López Fonseca, J. M., Muñíz Álvarez, J. L., García Calzón, J., Miranda Ordieres, A. J. and Fojón, D. 1998, Recent Res. Devel. Electrochem., 1, 281.
26. Hirotsu, M., Kojima, M., Nakajima, K., Kashino, S., Yoshikawa, Y. 1996, Bull. Chem. Soc. Jpn., 69, 2549.